Journal of Physics: Conference Series

Automatic system for estimating the volume of the left ventricle based on two-dimensional MRI images of the heart along the long axis

To cite this article: S.V. Porshnev *et al* 2018 *J. Phys.: Conf. Ser.* **944** 012092

Automatic system for estimating the volume of the left ventricle based on two-dimensional MRI images of the heart along the long axis

S.V. Porshnev, A.O. Bobkova, V.V. Zyuzin, A.A. Mukhtarov, M.A. Chernyshev, D. M. Akhmetov

Department of Information Technology and Automation UrFU, IRIT-RTF
Yekaterinburg, Russia

Abstract. The article is devoted to the development of a system that allows automatic estimation of systole, diastole and left ventricular ejection fraction of the heart based on the sequence of MRI images from the apical two-chamber and four-chamber positions. The implemented system was tested on the images of the heart of 200 patients, and its accuracy and operability was assessed. Keywords – left ventricle; final systolic volume; final diastolic volume; ejection fraction; magnetic resonance imaging; two-chamber projection; four-chamber projection; neural networks; recovery of volume

1. Introduction

In the practice of cardiac research, magnetic resonance imaging (MRI) is used, which allows the cardiologist to assess the functional state of the human heart muscle. For this purpose, on the basis of the analysis of MRI images, a specialist evaluates, usually manually, the change in the volume of the left ventricle of the heart (LV) and the ejection fraction (EF) of the LV (the ratio of the difference between the maximum (diastole) and minimum (systole) LV volumes to diastolic LV volume). As a result, the process of assessing the functional state of the heart muscle is very laborious. In this regard, the development of an automatic system for estimating LV volume based on MRI images is relevant.

The article describes an automatic system for recovering the volume of the LV based on two-dimensional images of the heart along the long axis.

2. Problem Definition

In the study of the heart muscle, MRI images of the heart are traditionally obtained in three projections: an apical two-chamber projection, an apical four-chamber projection, and a parasternal position of the short axis. In this connection, it is clear that the task of automatically estimating the volume of the LV based on MRI images can be decomposed into two independent tasks in accordance with the types of projections used: 1) projections along the long axis of the LV [1]; 2) projections along the short axis of the LV. In the studies carried out, projections on the long axis were used. In the course of solving the task, the following problems were identified and solved:

- Formation of a set of MRI images of the heart in selected projections.
- Transformation of MRI images into data suitable for training neural networks (NN).
- Choice of architecture of neural networks and their training.
- Selection of postprocessing methods for the results of processing MRI frames obtained at the output of the neural network.
- Evaluation of volume and EF of LV.
- Analysis of the results of the automatic system.

3. Main part

3.1. The structure of the source data

In the study, data was used on the competitive platform Kaggle [9]. They are a collection of more than 100.000 MRI images of more than 700 patients in the DICOM format. For the training of neural networks, MRI images of 500 patients were used, the remaining images were used to assess the quality of the work of the automated evaluation system. Examples of the two-chambered projection of the heart along the long axis and the four-chamber projection in the successive phases of one cardiac cycle are shown in Figure 1, 2, respectively.

3.2. Data preparation

3.2.1. Marking of MRI images For the training of neural networks, a pre-prepared set of data representing MRI frames was used, on which the areas corresponding to the LV were manually marked (Figure 3)

About 11.000 MRI frames were hand-marked in equal parts for a two-chamber and four-chamber projection.

3.2.2. Artificail increase in the data set Due to the fact that the set of 5500 images was insufficient for training the neural network and obtaining satisfactory estimates of LV volume, the original volume of MRI frames was artificially increased by the distorted versions of the original set [4]. This technique will increase the network's resistance to various shifts and rotations of the left ventricular contour on MRI images. To obtain distorted source images, we used affine transformations (mirror reflection with respect to oX and oY axes, shifts, rotations by a random angle in and counterclockwise, and also compression of the image along coordinate axes with a random compression ratio). The described affine transformations were applied simultaneously for both MRI frames and corresponding images obtained as a result of manual marking (Figure 4).

Figure 1. Sequence of frames of one cardiac cycle of a two-chamber projection of the heart along the long axis.

As a result, the original set of images was enlarged from 11.000 to 10^5 images. Further increase in the number of images was found to be inexpedient, since with a large number of MRI frames, the training time on the graphic card GTX 1060 was unacceptably large.

3.3. Architectures and learning outcomes of neural networks

The accumulated experience of using neural networks in visual recognition problems shows that with the task of isolating the contour of the left ventricle on biomedical images, deep convolutional NN are best able to cope [6], since they are able to assign a class label to each pixel separately [8]. In this connection, the FCN-8s [7] and UNET [10] architectures were used.

3.3.1. Modification of NN architectures Due to the fact that the FCN-8s architecture is designed to segment the image into 21 classes, which is redundant when the left ventricle area for which is redundant when the left ventricle area identification needs

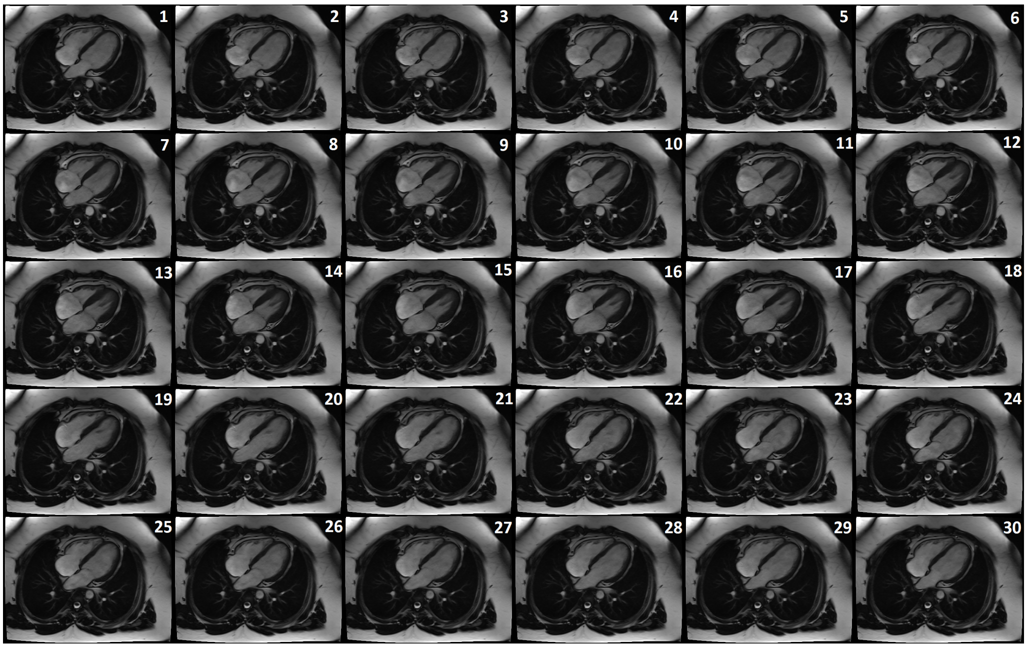

Figure 2. Sequence of frames of one cardiac cycle of a four-chambered projection of the heart along the long axis.

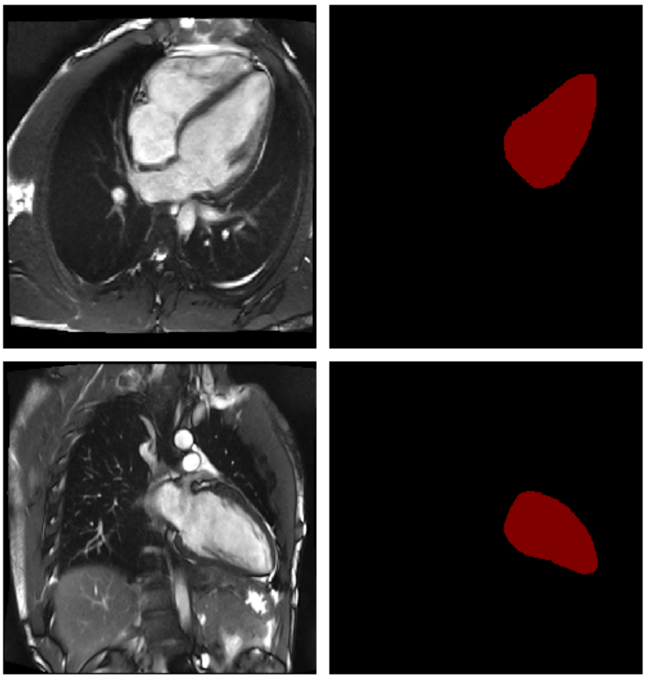

Figure 3. Results of marking MRI images: from above – four-chamber projection, from below – two-chamber projection.

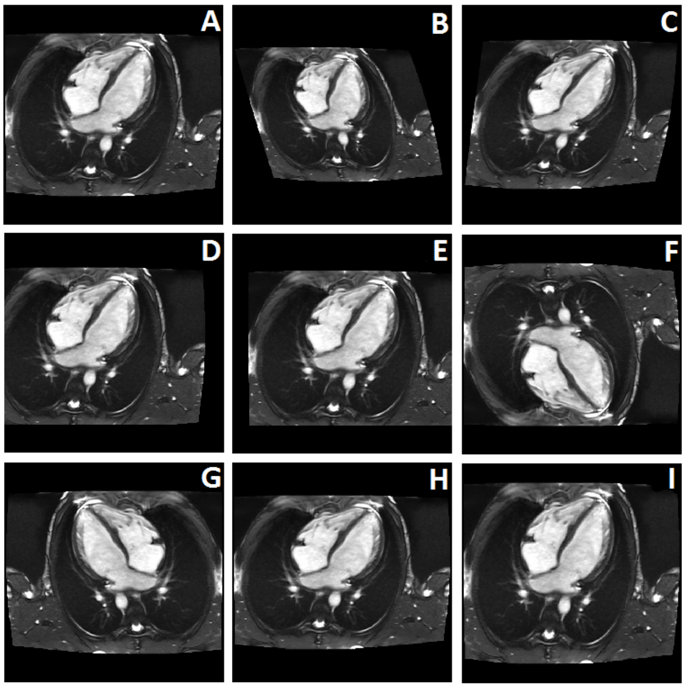

Figure 4. Affine transformations: A – original image, B – slope to the left, C – slope to the right, D – random shift, E – random shift, F – reflection along the x axis, G – reflection along the y axis, H – compression along the x, I – compression along the y.

only 2 classes (background and LV area). A new layer has been added to the network architecture, allowing the neural network to make a prediction for two classes. The introduction of a new layer allowed the used NN to find the region of the LV using information about the background and area of the LV.

Due to the fact that at the output of the NN of UNET architecture the image is smaller than the input one, therefore the UNET architecture was modified by introducing an additional layer, which provided an increase in the size of the input image by 92 pixels from each side by means of mirror reflection.

To prevent the overfitting of the NN with the FCN-8s architecture, the regularization method – dropout, which was located in the two lower full-connected layers was used (the coefficients used in this method were chosen equal to 0.5). Implement an analog approach for a NN with the UNET architecture failed due to insufficient video memory.

Also additionally, in the architecture of both NN, a layer is added that provides the calculation of the metric used to estimate the accuracy:

$$dice = \frac{2 \times |P \times T|}{|P|^2 + |T|^2}, \tag{1}$$

where P – network prediction, T – true image.

3.3.2. Selecting the values of the hyperparameters of the NN The following settings of the hyperparameters of the NN were used in the studies:

- base_lr – 0.0001.
- lr_policy – step.
- training_epochs – 10.
- weight_decay – base_lr / 100.
- type – Adam.
- momentum – 0.9.

whose values were selected experimentally, based on an analysis of the values of the coefficient dice, calculated in accordance with equation 1.

3.3.3. Refinement of the estimination of the probability of the pixel belonging to the region of the LV To correct the values of the probability of belonging pixels to the LV areas, the weighted average probabilities of the LV pixel area belonging to the FCN-8s (0.55 weight coefficient) and UNET (0.45 weight coefficient) neural networks were calculated [5]. The values of the weight coefficients were chosen experimentally.

3.3.4. Learning outcomes of NNs Training of neural networks was carried out in Caffe [2] framework with graphical shell DIGITS.

As a result of training, the following models of deep convolutional NNs were obtained:

- The model, trained on a data set with an apical two-chamber projection and based on the FCN-8s architecture.
- A model trained on a set of data with an apical two-chamber projection and based on the UNET architecture.
- The model, trained on a data set with an apical four-chamber projection and based on the FCN-8s architecture.
- The model, trained on a data set with an apical four-chamber projection and based on the UNET architecture.

3.4. Postprocessing

3.4.1. Removing faulty areas identified using NNs The analysis of LV areas manually processed by MRI images showed that the minimum size of the LV image in both the two-chamber and the four-chambered projection always exceeded 400 pixels. In this connection, objects allocated with a NN with an area of less than 300 pixels were considered erroneous and were removed from the binary image [3] (Figure 5).

2017 IEEE Dynamics of Systems, Mechanisms and Mahines (Dynamics) (Omsk, Russia) 14 Nov–16 Nov 2017

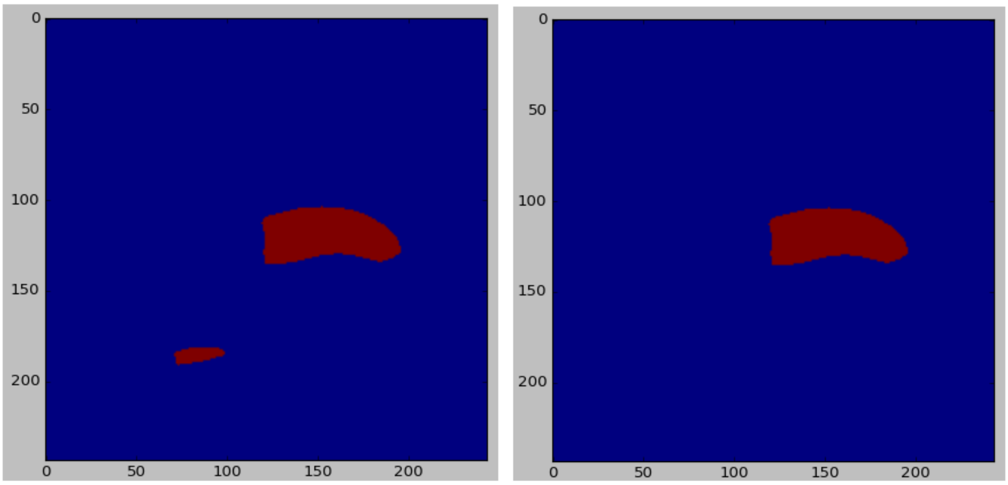

Figure 5. Example of deleting mistakenly identified areas on a binary image.

3.5. Evaluation of the volume of the LV

3.5.1. Calculation of finite volumes using an ensemble of neural networks To obtain LV volume estimation, the modified Simpson method [11] was used, the illustration of which is shown in Figure 6.

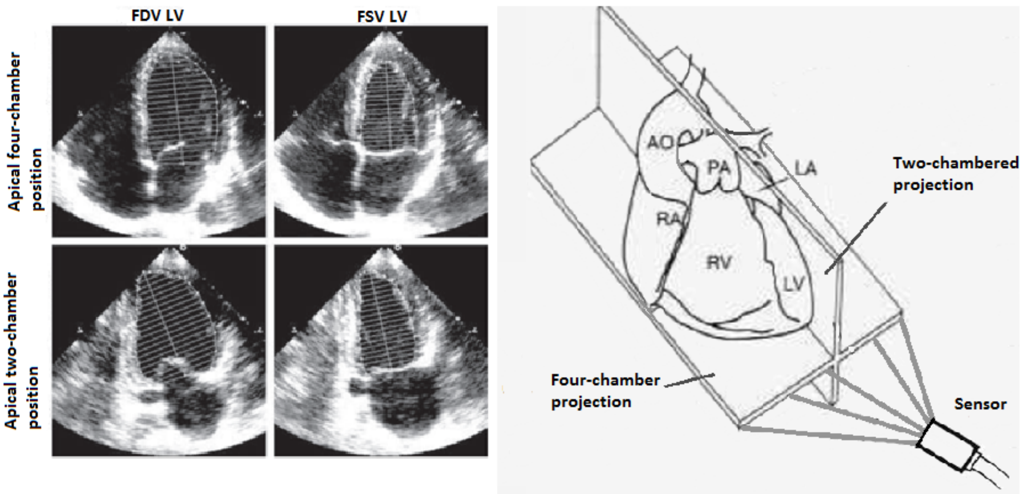

Figure 6. Modified Simpson method.

This method was applied to each of the frames MRI-film, the duration of which corresponded to the duration of one cardiac cycle. Further, the diastolic (maximal) and systolic (minimal) volumes of the LV were determined from the obtained time series containing the "instantaneous values" of the volume of the left ventricle.

3.6. Elimination of a systematic error in estimates of LV volume and EF

The analysis of the volume values on a sample of data used for training neural networks revealed the difference between these estimates and similar expert estimates. From a mathematical point of view, the differences between the automatically determined values of the volumes of the LV and the corresponding expert values, as well as between the EF calculated by these volumes, represent some samples of the random variables presented in Figure 7.

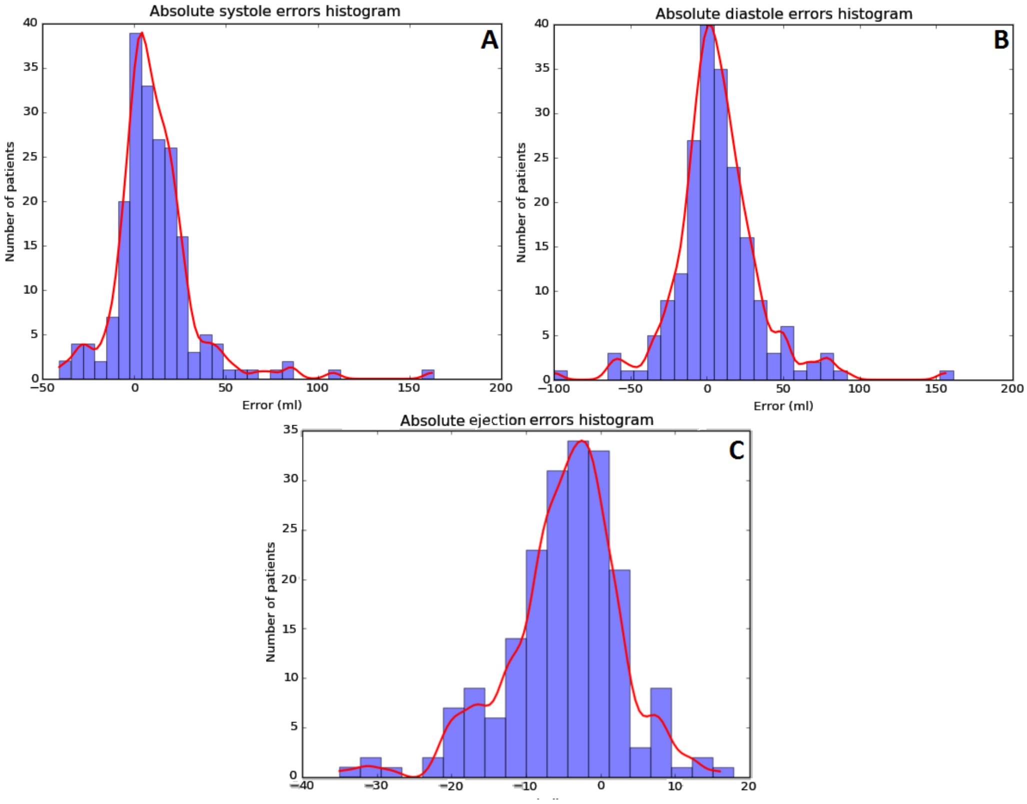

Figure 7. System operation results before calibration: A – histogram of error distribution of estimates of systolic volume, B – histogram of error distribution of estimates of diastolic volume, C – histogram of error distribution of emissions fraction estimates.

It can be seen from Figure 7 that the maximum of the distribution density, the discussed random sample samples are reached at the following points: 0.8 ml (diastolic volume), 4.4 ml (systolic volume), -2.5% (EF), which are estimates of the systematic error of diastolic, systolic values and EF. In the future, the calculation of the ejection fraction was preceded by the removal of the obtained estimates of the corresponding values of the systematic errors from the values of the systolic and diastolic volumes.

Table 1. Comparison of received results

Id	Systole(ml)		Diastole(ml)		Ejection fraction(%)	
	Received	Expert	Received	Expert	Received	Expert
501	84.58	104.30	186.08	212.50	54.55	50.92
521	78.24	58.30	189.15	165.80	58.64	64.84
541	47.79	45.40	122.04	116.20	60.84	60.93
561	75.78	54.50	186.24	158.00	59.31	65.51
581	14.91	8.00	19.55	19.00	23.73	57.89
601	66.67	73.00	175.00	176.60	61.90	58.66
621	34.14	65.80	96.40	139.90	64.59	52.97
641	97.18	104.30	209.59	234.20	53.63	55.47
661	87.26	94.20	161.31	173.80	45.91	45.80
681	35.29	32.60	71.14	84.00	50.39	61.19
700	77.25	57.50	135.39	114.7	42.94	49.87

4. Analysis of the results

Consider the results obtained with the use of an automatic system for estimating the volume of the LV. Table 1 presents the results of systolic, diastolic volumes and EF for 11 patients.

From table 1 it can be seen that the expert and automatic values are close enough to each other. The discrepancy between the values of the ejection fraction does not exceed 12 percent. Analysis of similar data obtained for all patients showed that only one patient had an EF that differed from the expert value by more than 30%. An analysis of this patient's MRI film that the frames of this film are of inadequate quality.

Histograms of differences in expert estimates of systolic and diastolic volumes and EF and similar estimates obtained automatically are presented in Figures 8, 9, 10.

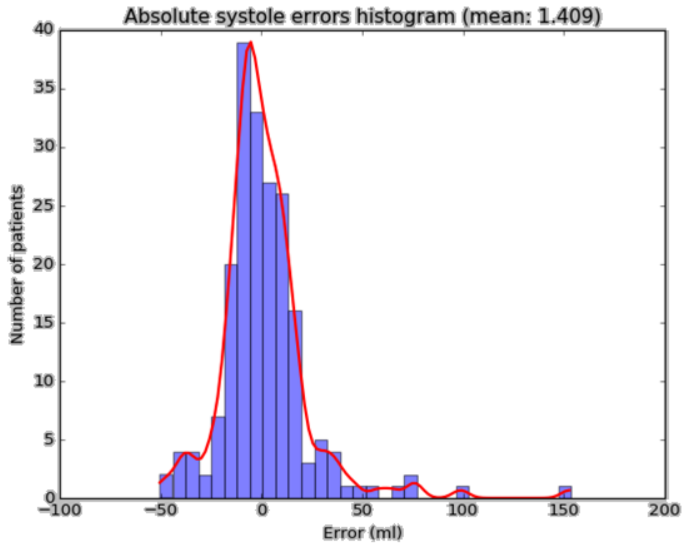

Figure 8. Histogram of error distribution of estimates of systolic volume.

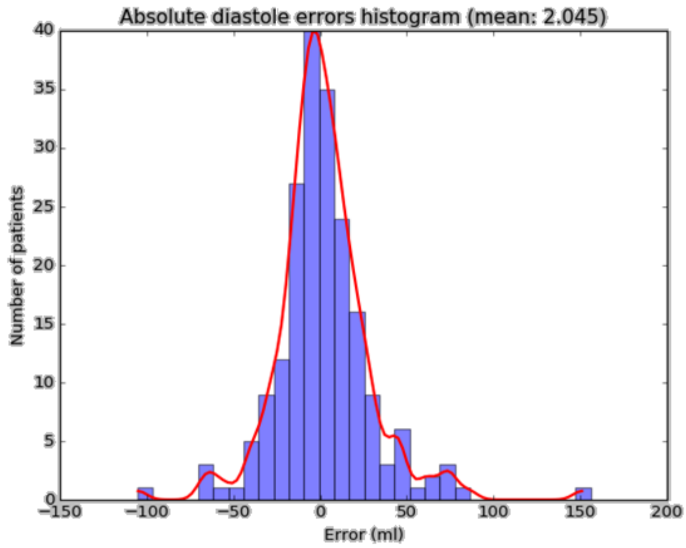

Figure 9. Histogram of error distribution of estimates of diastolic volume.

It can be seen from Figures 8, 9, 10 that the maxima of the distribution densities of the differences under consideration are reached at points with abscissa equal to 0. This indicates that there is no systematic bias of automatically obtained estimates of diastolic, systolic volumes and EF.

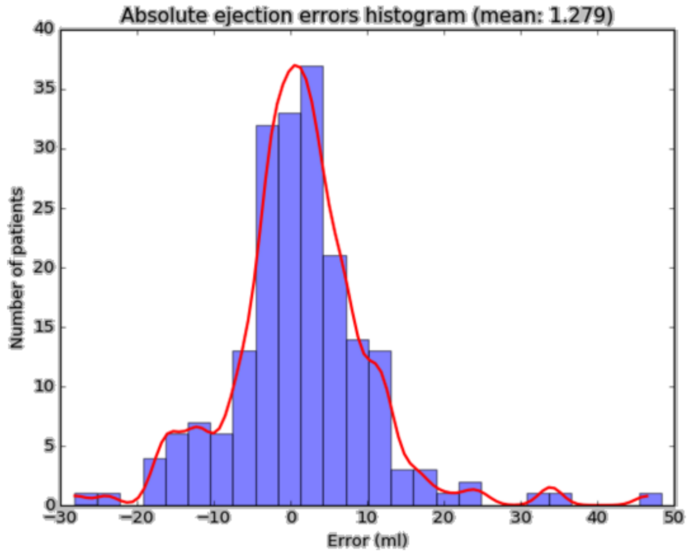

Figure 10. Histogram of error distribution of emissions fraction estimates.

Conclusions

The developed automatic system of volume estimation of the LV of the heart on the basis of the analysis of two-dimensional MRI images of two-chamber and four-chamber projections along the long axis with the use of NNs demonstrated its efficiency. A more detailed study of the statistical properties of the errors in the systolic and diastolic volumes of the ejection fraction is the subject of subsequent publications.

References

[1] Automatic Left Ventricle Detection in MRI Images Using Marginal Space Learning and Component-Based Voting [Electronic resource]. – Access mode: `https://www.umiacs.umd.edu/ zhengyf/LV_Detection_MRI_SPIE09.pdf`
[2] Caffe — Layer Catalogue [Electronic resource]. – Access mode: `http://caffe.berkeleyvision.org/tutorial/layers.html`
[3] Deep Learning for Medical Image Segmentation [Electronic resource]. – Access mode: `https://arxiv.org/pdf/1505.02000.pdf`
[4] Diagnosing Heart Diseases in the Data Science Bowl [Electronic resource]. – Access mode: `http://blog.kaggle.com/2016/04/13/diagnosing-heart-diseases-with-deep-neural-networks-2nd-place-ira-korshunova`
[5] Ensemble learning [Electronic resource]. – Access mode: `http://www.scholarpedia.org/article/Ensemble_learning`
[6] Estimating the volume of the left ventricle from MRI images using deep neural networks [Electronic resource]. – Access mode: `https://arxiv.org/pdf/1702.03833.pdf`
[7] Fully Convolutional Networks for Semantic Segmentation [Electronic resource]. – Access mode: `https://arxiv.org/pdf/1605.06211.pdf`
[8] How do Convolution Neural Networks work? [Electronic resource]. – Access mode: `https://brohrer.github.io/how_convolutional_neural_networks_work.html`

2017 IEEE Dynamics of Systems, Mechanisms and Mahines (Dynamics) (Omsk, Russia) 14 Nov–16 Nov 2017

[9] Second Annual Data Science Bowl [Electronic resource]. – Access mode: https://www.kaggle.com/c/second-annual-data-science-bowl
[10] U-Net: Convolutional Networks for Biomedical Image Segmentation [Electronic resource]. – Access mode: https://arxiv.org/pdf/1505.04597.pdf
[11] Recommendations on the quantification, structure and function of the heart chambers [Electronic resource]. – Access mode: http://webmed.irkutsk.ru/doc/pdf/echo.pdf